Origins of Open-Channel Noise in the Large Potassium Channel of Sarcoplasmic Reticulum

ATTICUS H. HAINSWORTH, RICHARD A. LEVIS, and ROBERT S. EISENBERG

From the Department of Molecular Biophysics and Physiology, Rush Medical Center, Chicago, Illinois 60612

ABSTRACT Open-channel noise was studied in the large potassium channel of the sarcoplasmic reticulum (SR). Inside-out patches were excised directly from the SR of split skeletal muscle fibers of lobster, with lobster relaxing ringer (LRR) in bath and pipette. The power spectrum of open-channel noise is very low and approximately flat in the 100 Hz–10 kHz frequency range. At 20°C, with an applied voltage of 50 mV, the mean single-channel current $\langle i \rangle$ is 9 pA (mean single-channel conductance = 180 pS) and the mean power spectral density 1.1×10^{-29} A^2/Hz. The latter increases nonlinearly with $\langle i \rangle$, showing a progressively steeper dependence as $\langle i \rangle$ increases. At 20 mV, the mean power spectral density is almost independent of $\langle i \rangle$ and ~1.4 times that of the Johnson noise calculated for the equivalent ideal resistor with zero net current; at 70 mV it increases approximately in proportion to $\langle i \rangle^2$. The mean power spectral density has a weak temperature dependence, very similar to that of $\langle i \rangle$, and both are well described by a Q_{10} of 1.3 throughout the range 3–40°C.

Discrete ion transport events are thought to account for a significant fraction of the measured open-channel noise, probably ~30–50% at 50 mV. Brief interruptions of the single-channel current, due either to blockage of the open channel by an extrinsic aqueous species, or to intrinsic conformational changes in the channel molecule itself, were a possible additional source of open-channel noise. Experiments in modified bathing solutions indicate, however, that open-channel noise is not affected by any of the identified aqueous species present in LRR. In particular, magnesium ions, the species thought most likely to cause brief blockages, and calcium and hydrogen ions, have no detectable effect. This channel's openings exhibit many brief closings and substates, due to intrinsic gating of the channel. Unresolved brief full closings are calculated to make a negligible contribution (< 1%) to the measured power spectral density. The only significant source of noise due to band width-limited missed events is brief, frequent 80% substates (mean duration 20 μs, mean frequency 1,000 s^{-1}) which account for a small part of the measured power spectral density (~14%, at 50 mV, 20°C).

Address correspondence to Dr. Eisenberg, Department of Molecular Biophysics and Physiology, Rush Medical Center, 1750 West Harrison Street, Chicago, IL 60612.

Dr. Hainsworth's present address is Section of Physiology, School of Biological and Chemical Sciences, University of Greenwich, London SE18, UK.

J. GEN. PHYSIOL. © The Rockefeller University Press · 0022-1295/94/11/0857/27 $2.00
Volume 104 November 1994 857–883

We conclude that a large fraction of the measured open-channel noise results from intrinsic conductance fluctuations, with a corner frequency higher than the resolution of our recordings, in the range 10^4–10^7 Hz. We infer the presence of motions within the channel molecule in this frequency range.

INTRODUCTION

Open-channel noise means any fluctuation in a single-channel current recording that is present only when the channel is open. Gaussian, apparently continuous current fluctuations are seen in the nicotinic end-plate channel (Sigworth, 1985) and in a stretch-activated cation channel (Eisenberg, Hainsworth, and Levis, 1987). These are thought to reflect fluctuations in the channel conductance, as a result of vibration within the channel molecule. In addition, discontinuous step changes in conductance are seen in many channels, due either to gating transitions (subconductance states and brief closings) or to blockage of the open channel by an extrinsic molecule (for discussion, see Hille, 1992). These discontinuous changes, if too brief to be resolved by the recording system, will add to the observed open-channel noise (Sigworth, Urry, and Prasad, 1987; Heinemann and Sigworth, 1988, 1989). Finally, a small, unavoidable noise in any current arises from the discrete nature of the charge carriers and their thermal energy. This discrete transport noise is described under different conditions as Johnson, thermal, Schottky or shot noise (Oliver, 1965; van der Ziel, 1970; see Appendix). Discrete transport noise reflects the ion transport mechanism, in that its power spectrum is determined by the potential energy profile of the conducting pathway, and the manner in which ions diffuse through it (Frehland, 1978; Heinemann and Sigworth, 1990).

The SR potassium channel studied here was chosen for two reasons. First, its high conductance and very long burst durations favor power spectral measurements. Second, a large body of previous work (reviewed in Miller, Bell, and Garcia, 1984; Levitt, 1986, Hladky, 1989) strongly indicates that it contains only one ion at a time, under most conditions. Thus, it is expected to have a relatively simple transport mechanism. Our aim was to determine the power spectrum of open-channel noise in this channel and to analyze the contributions from different sources of noise. Parts of this work have been reported previously (Eisenberg, Hainsworth, and Levis, 1988, 1989; Hainsworth, Tang, Wang, Levis, and Eisenberg, 1988; Hainsworth, 1989).

METHODS

Preparation

Lobsters (*Homarus americans*) were killed by decapitation and the remotor muscle of each second antenna removed intact. This muscle contains ~70% by volume of SR, with very sparse contractile filaments (Tang, Wang, and Eisenberg, 1989). Single fibers were dissected and split open in Lobster relaxing Ringer (LRR) as described by Tang et al. (1989). Patches were excised from the exposed, upward-facing interior of the split fiber, presumed to contain much SR. In all experiments, single channels were recorded in inside-out patches with identical solutions in both bath and pipette. Pipettes were made from Corning No. 7052 glass and coated with Sylgard 184® (Dow Corning Co., Corning, NY). After excising a patch, a constant voltage, usually ~2

mV in magnitude, was added to null all single-channel currents. Applied voltages quoted are pipette potentials relative to this reference. No correction was made for the small voltage (< 1 mV) dropped over series resistance (typically 20 MΩ). The bath temperature was held constant by Peltier units.

Solutions

LRR contains (in millimolar): 460 potassium glutamate (Sigma grade, 99–100%), 1.2 $CaCl_2$, 1.0 $MgCl_2$, 1.0 MgATP (Sigma Immunochemicals, St. Louis, MO), 5.0 EGTA, 25 HEPES, pH 7.0 (total K: 480 mM). The calculated free Ca^{2+} concentration is ~100 nM, and free Mg^{2+} ~1 mM. In low Mg solution, $MgCl_2$ and MgATP were omitted and the total magnesium content is 0.005 mM, determined by atomic absorption spectroscopy (Biotrace Labs, Salt Lake City, UT). In low Ca solution, $CaCl_2$ and MgATP were omitted, and only 1.0 mM EGTA was present. Both low Mg and Low Ca solutions were adjusted to pH 7.0. A low H solution was made by adding 1 M KOH to LRR, to pH 8.0–8.3 (total K: 495 mM). HEPES (pK_a = 7.5) is still an adequate buffer in this solution. The calculated free Ca^{2+} of this solution is 2 nM and the calculated free Mg^{2+} is 0.5 mM. All solutions were made in Millipore water (Millipore Corp., Bedford, MA) (> 10 MΩcm resistivity) and had a measured osmolarity in the range 920–940 mosm.

The Recording System

Constant voltage commands were applied to the pipette for many seconds and steady state single-channel activity recorded using an Axopatch® patch clamp (Axon Instruments, Foster City, CA). The patch clamp had an intrinsic frequency response of 20 kHz and a 10–90% rise time of 20 μs. Band widths quoted are always from DC to upper −3 dB frequency. The patch clamp output was filtered at 20 kHz (8-pole Bessel LPF902, Frequency Devices Inc., Haverhill, MA) and recorded continuously on magnetic tape, using a digital audio processor (PCM-501-ES) with 16-bit resolution. Within these promising stretches, regions of single-channel data were selected for power spectral estimation by the automated process described below. All data analysis programs were run on a Celerity 1200 computer. Sampling by the PCM was at 44.1 kHz sampling rate, and a video cassette recorder (Sony Betamax system). Played-back signals passed through a 20-kHz Cauer elliptic filter (inside the PCM unit) then a 10-kHz 21-pole Chebychev filter (Allen Avionics Inc.). Promising stretches of ~10-s duration were selected by eye and redigitized at 25 kHz, using a Data Translation 2827 A/D board with 16-bit resolution, then analyzed on a Celerity 1200 computer. Sampling by the PCM-501 unit at 44.1 kHz was found to introduce slight aliasing at high frequencies (Brigham, 1974): the power spectral density at 10 kHz was too high by a factor of 1.06. Further aliasing is not likely to be added on redigitizing, thanks to the very sharp cut-off of the Cauer and Chebychev filters.

In some recordings, a capacitative feedback headstage was used (IHS-1, Axon Instruments) with 30-kHz frequency response and 10-μs rise time. Here, the patch clamp's output was filtered at 10 kHz (8-pole Bessel) then sampled at 44.1 kHz with negligible aliasing and, on playing back, redigitized at 50 kHz with no other filtering than the 20 kHz Cauer filter at the output of the PCM-501 unit.

Power Spectral Estimation

Power spectra were computed from periods when either only one channel was open, or no channels were open, selected by an automated process. Typically ~100 spectra were taken from each state, from ~10 s of data each, all within ~1 min. The open-channel noise power spectrum was then given by subtracting the average no-channels spectrum from the average one-channel spectrum (Sigworth, 1985). The no-channels noise is an estimate of the background noise from all sources other than the channel itself. This background noise

spectrum varied widely from patch to patch, but varied little over the lifetime of any one patch: no consistent variation with voltage or temperature was seen.

A step-detection algorithm (Kirlin and Moghadamjoo, 1986) located transitions between conductance states. The true current amplitude in a period between successive transitions was defined as the median of all points in that period (Fig. 1 *C*). Ideally, only changes in conductance state should remain in this trace, with all the Gaussian noise eliminated. The sample median is less sensitive than the sample mean to the presence of wild points, such as brief closings and substates, in Gaussian noise. While this true current record lay within a narrow range (usually between 0.2 and 0.6 pA wide) predefined by the user, the channel was considered to be in its main conductance state, and the data accepted. Background noise regions were selected in an analogous way. On inspection, obviously aberrant selections were manually deleted.

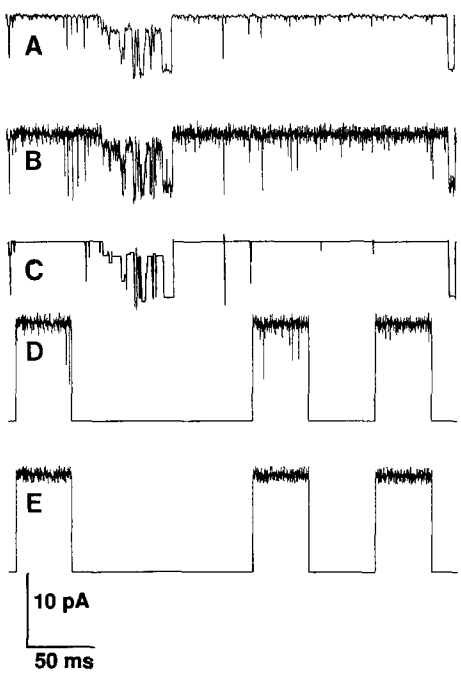

FIGURE 1. Automated data selection of single-channel currents from an inside-out patch at 20°C, pipette voltage = +50 mV. Channel closings are downward deflections: $\langle i \rangle$ = 9.0 pA (no full closing is present in this record). All traces show the same stretch of data at different stages of the selection process. (*A*) filtered at 1 kHz with a digital 8-pole Bessel filter, for illustration only. (*B*) Full band width data (10 kHz, 20 μs/point). The open-channel noise RMS is ~0.5 pA. (*C*) Transitions detected by the running window program. The median current between detected transitions is shown. Events briefer than ~400 μs are not detected. When the median current lies within a narrow amplitude range the data is selected (the range was 0.3 pA wide in this example). (*D*) Three blocks of 41-ms duration selected from *B* to compute power spectra. The connecting line is simply the reference level of the *A–D* converter. (*E*) The same three blocks as in *D*, after the masking program has removed brief excursions.

Blocks of sequential points, 41 ms in duration (1,024 data points, sampled at 25 kHz, or 2,048 at 50 kHz) were taken from the regions selected by the step detection algorithm to compute power spectra. Data points within 400 μs of a detected transition were avoided. Interruptions briefer than ~400 μs were not detected by the step-detection program, so a masking program (Sigworth, 1985) was used to remove them. Here, any data points lying outside 2.5 standard deviations from the median were identified as outliers and multiplied by zero (masked). This was repeated until no new outliers were found. On average, 3% (never more than 5%) of open-channel data were masked in this way, and 1.9% of background data. Power spectra were not corrected for the number of masked points.

Each 41-ms block selected was multiplied by a data window function (Papoulis, 1973) and its length doubled by adding terminal zeros, to increase the spectral frequency resolution. Its discrete Fourier transform (Brigham, 1974) was then computed by a fast Fourier transform

routine (NAG, Ltd., Oxford, UK) and the power spectral density given by the squared magnitude of the emerging complex numbers. The mean of many such spectral estimates was computed and the average open channel and average background noise power spectra subtracted, point by point. Average power spectra were divided by the transfer function of the recording system, before subtraction. The transfer function was obtained by applying a white noise signal (0–50 kHz) from a signal generator (Hewlett Packard 3722A) directly to the patch clamp input.

Spectra were plotted over the range 100 Hz–10 kHz (points 9–822) on a double logarithmic scale. At high frequencies, local averages over several neighboring points were plotted, ±1 local standard deviation. Some figures show mean power spectral density ± 1 SD over all points in the range 300 Hz–3 kHz (points 24–244).

Test of the Power Spectral Measurement

The above spectral estimation methods were applied to simulated data of known parameters. To represent background noise, current was recorded from a 20 MΩ pipette, driven into a Sylgard® disk to give a stable resistance of 7 GΩ. To represent brief closings, a random binary signal was synthesized on the computer (with mean closed time τ = 100 μs, mean frequency of occurrence λ = 100 s^{-1} and amplitude = 9 pA) then filtered with a 10 kHz digital 8-pole Bessel filter. To represent open-channel noise, analogue white noise (0–50 kHz) from a signal generator was applied to the patch clamp input, recorded in the usual way and scaled appropriately to give a mean power spectral density (±1 SD) of 2.9 (±0.3) × 10^{-30} A^2/Hz in the range 300 Hz–3 kHz. These three digital signals, when added together, gave a composite signal resembling raw open-channel data. This composite signal and the background noise were then both processed in the same way as experimental data. On average, 3.1 and 1.9% of points were masked in the composite and background noise signals respectively. The result of subtracting the two average power spectra was approximately flat, with a mean power spectral density of 2.4 (±0.8) × 10^{-30} A^2/Hz, which is 80% of the true value. An identical result was obtained when the simulated random binary events were not included in the composite signal. This indicates that the masking program effectively removes brief closings but in addition, truncates some Gaussian noise excursions, thus depressing the mean power spectral density from its correct value.

When the threshold for masking was 3.0 SDs from the median, subtracted spectra obtained from experimental data were higher than those obtained with 2.5 SD thresholds, by a factor of ~1.3. More closings and substates were found to be missed by the masking program with 3.0 SD thresholds, on inspection of masked records. Given the frequent closings and substates of this channel, it was decided to err on the side of stringency, to minimize the number of missed brief events. Assuming the error due to truncation of Gaussian noise to be roughly constant, this suggests that the mean power spectral densities given below are ~80% of the true ones for Gaussian open-channel noise.

Duration Histograms

The kinetic parameters of brief, full closings were determined, likewise those of brief excursions to a substate of amplitude 80% of the main conductance state. For kinetic analysis, data were usually recorded using the capacitative feedback headstage and sampled at 50 kHz, with the recording system dominated by a 10 kHz 8-pole Bessel filter (LPF902) giving a 10–90% rise time of 40 μs with negligible overshoot or ringing. Dwell times were given by a simple threshold-crossing algorithm. To detect full closings, the threshold was placed half way between the main open and closed peaks in an amplitude histogram of the data at full band width. Around threshold crossings, points were interpolated fourfold using a cubic-spline routine

(Colquhoun and Sigworth, 1983) to give a resolution of 5 μs/point. The probability density $f(t)$ of an exponential population of lifetimes is:

$$f(t) = \lambda\tau^{-1}e^{-t/\tau} \quad (1)$$

where λ is the mean frequency of events per second and τ is the time constant of the population, equal to the mean event lifetime. Closed times were binned and plotted as $\log_{10}$ [events·s^{-1}·bin^{-1}] vs duration. In this form, exponential components that are well separated can be described by a simple straight line fit. In the histograms in Figs. 8 and 10 the bins for events <30 μs show a decline, indicating that events were missed.

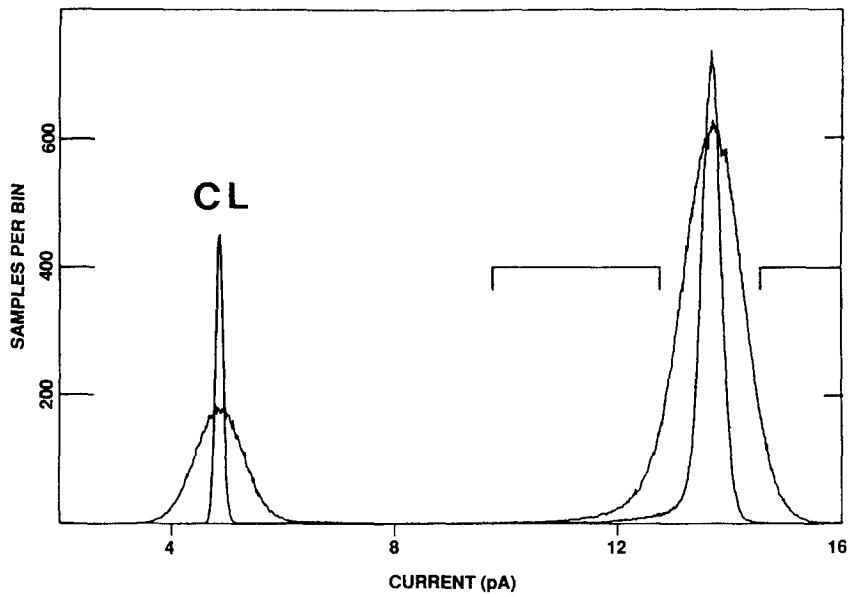

FIGURE 2. Amplitude histograms of 10 s of data, both at 10 kHz band width (262 bins/pA) and after digital Bessel filtering at 1 kHz (655 bins/pA): the narrower peaks come from the 1 kHz data. (*CL*) Closed state. Pipette voltage = +50 mV, $\langle i \rangle$ = 9.0 pA. The peak current amplitude is 13.65 pA at 10 kHz. Horizontal braces mark the ranges used for estimating duration histograms of brief 80% substates, by the subtraction method described in the text. The main thresholds (90%, 110%) are 0.9 pA from the peak current amplitude. The secondary thresholds (60%, 140%) are 3.9 pA from the peak current amplitude (only part of the upper range being shown).

Excursions to the 80% amplitude substate were ~2 pA in amplitude and so brief that they had to be examined at full 10-kHz band width, when the background noise was typically 0.5 pA RMS. The distribution of their dwell times was estimated as follows. A threshold was placed at 90% of the main current amplitude (equivalent to the half-amplitude position of the 80% substate) and a second threshold at 60%, as determined from an amplitude histogram (Fig. 2). A duration histogram was made for events that left the main conductance state to cross the first threshold, then recrossed it without reaching the second one.

Using this criterion, many brief 80% amplitude transitions were sampled, but also many extraneous noise excursions. To correct for the latter, a second dwell-time histogram was made,

with thresholds at 110 and 140% (i.e., at equivalent positions on the other side of the main current amplitude). The unwanted noise excursions were assumed to be symmetrical about the main current level; so the second histogram was subtracted from the first, bin by bin, to give an estimate of the true duration histogram for brief 80% substates (Fig. 10). In Fig. 10, the subtraction had a minimal effect on bins above ~50 μs. As a test, this method was applied to artificial data with known parameters. A data file containing noiseless 2-pA pulses with single-exponential distributions of open and closed times was generated by computer, with τ = 28 μs and λ = 1,000 s^{-1}. The pulses were digitally filtered (10 kHz, 8-pole Bessel) to be comparable to experimental data, then added to a recording of background noise (0.5 pA RMS) from an experiment. The duration histogram obtained by the above subtraction method gave τ_{fit} = 25 μs and λ_{fit} = 1,300 s^{-1} by a simple least squares fit. These were considered adequate approximations.

RESULTS

The channel type most often seen in these patches strongly resembles the SR potassium channel studied in reconstituted preparations (reviewed in Miller et al., 1984) and in blebs of native SR membrane (Stein, Nelson, and Palade, 1989). It has a mean single-channel conductance of ~180 pS with a linear current-voltage relation in the ±80 mV range (Tang et al., 1989). Its openings last for many seconds (Fig. 1) but are punctuated with many brief (<1 ms) closings and substates. Closings lasting longer than 1 s occur infrequently. Unless stated otherwise, all results come from inside-out patches at 20°C, with identical solutions of LRR in bath and pipette and an applied voltage of 50 mV amplitude.

The Power Spectrum of Open-Channel Noise Is Flat and Low

Examples of average power spectra from unsubtracted one-channel noise and background noise are shown in Fig. 3 *A*. Subtracting the latter from the former is assumed to give the power spectrum of open-channel noise (Fig. 3 *B*). In the 100 Hz–10 kHz frequency range, the power spectral density of subtracted open-channel noise is approximately constant: no corner frequency is detectable. Most subtracted power spectra have a $1/f^{\alpha}$ trend, where α is small, positive and variable between experiments (typically α = 0.2, Figs. 3 and 4). The origin of this trend is unknown, but it was more pronounced when a greater percentage of points had been masked.

The mean power spectral density is very low. With an applied voltage of 50 mV, the mean single-channel current $\langle i \rangle$ was 9 pA and the mean power spectral density 10.7 ± 3.2 × 10^{-30} A^2/Hz (n = 4). At 20 mV, $\langle i \rangle$ = 3.6 pA and the mean power spectral density exceeds by a factor of 1.5 that given by the Johnson formula (Eq. 14) for an ideal 5.6 GΩ (180 pS) resistor at equilibrium.

The low and high-frequency extremes of the subtracted power spectrum are variable between recordings so the mean power spectral density is computed only over the range 300 Hz–3 kHz. Multiple factors underly the variability. At the high frequency end: (*a*) background noise dominates open-channel noise, so the spectral subtraction (Figs. 3, *A* and *B*) is less reliable; (*b*) a small degree of aliasing is present (<6%, see Methods); (*c*) the correction for the recording system's transfer function (see Methods) is not perfect, and this error will be felt most at high frequencies, close to the upper −3 dB frequency. At the 100 Hz end: (*a*) harmonics of residual

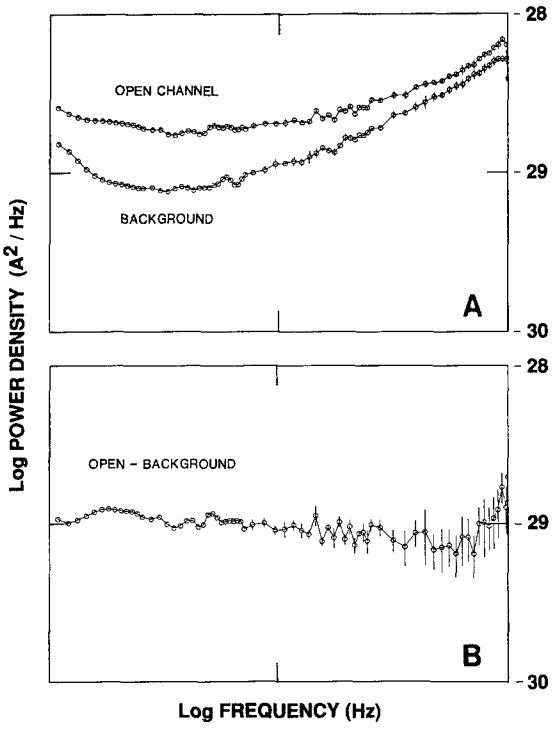

FIGURE 3. Power spectra of open-channel and background noise, pipette voltage = −50 mV, $\langle i \rangle$ = 9.2 pA. (*A*) Average power spectrum from 588 1,024-point discrete Fourier transforms over a period of 35 s from the main-channel conductance state and 171 transforms from background noise in the same patch. (*B*) The power spectrum of open-channel noise, obtained by subtracting the two spectra in *A*. In this example, mean power spectral density = 9.3 ± 1.4 × 10^{-30} A^2/Hz (over the frequency range 300 Hz–3 kHz).

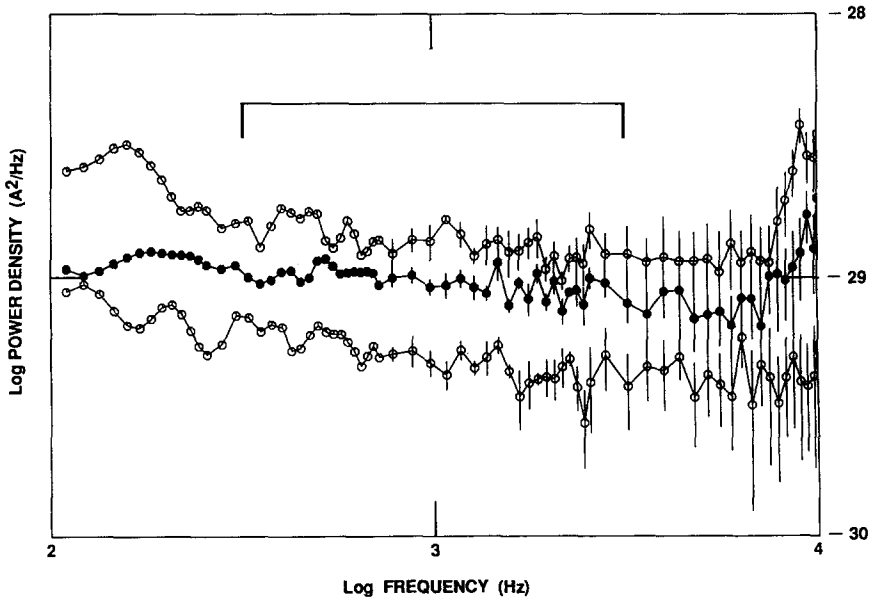

FIGURE 4. Power spectra with increasing $\langle i \rangle$. From the top, pipette voltage = −70, −50, −20 mV and $\langle i \rangle$ = 12.9, 9.2, and 3.9 pA, respectively. Each spectrum came from a different patch, under similar recording conditions. The middle curve is that of Fig. 3 *B*. The horizontal brace marks the 300 Hz–3 kHz range over which mean power spectral density was computed.

oscillations below 100 Hz, such as the 60 Hz mains supply, may elevate neighboring frequencies; (*b*) a $1/f^{\beta}$ component is visible in some spectra at low frequencies, with $\beta \approx 1$ (not shown). This low-frequency $1/f^{\beta}$ component is not reproducible and may be due to imperfect rejection of unwanted gating events. The low-frequency limit of the power spectra shown here (24 Hz) is imposed by the gating behavior of the channel: sojourns in the main conductance state longer than 41 μs (=1/24 Hz) are too rare for enough spectral estimates to be obtained.

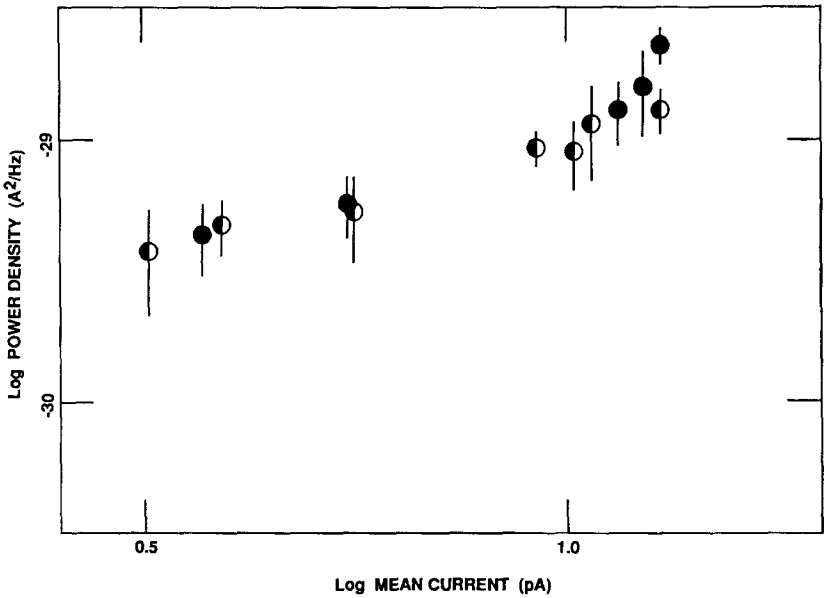

FIGURE 5. Mean power spectral density increases with $\langle i \rangle$. Data from seven patches. Each power spectrum came from >24 (and usually >100) open-state transforms. For the first three points from the left, pipette voltage was +20 mV (*filled symbols*) or −20 mV (*open symbols*), in the next two, 30 mV, the next four, 50 mV, and the last three, 70 mV. Note that log 3 = 0.50, so an abscissa value of 0.5 corresponds to 3 pA. The Johnson formula noise level is $\sim 3 \times 10^{-30}$ A^2/Hz, corresponding to −29.5 on the vertical axis.

Mean Power Spectral Density Increases with Mean Single-Channel Current

When higher voltages are applied, both $\langle i \rangle$ and the power spectral density of open-channel noise increase (Figs. 4 and 5). The current dependence of open-channel noise is not a simple power-law relation in that the data points on the double logarithmic plot in Fig. 5 clearly do not lie on a straight line of constant slope. In the limit of diminishing $\langle i \rangle$, the slope is close to zero. At the upper limit of the measured range of $\langle i \rangle$, the slope is close to 2, though from Fig. 5 it is not possible to say whether this is the maximum slope. With applied voltages of the same magnitude but opposite polarity, the power spectra obtained are very similar (not shown). The single-channel conductance and open probability are also only very weakly voltage sensitive (Tang et al., 1989).

The Temperature Dependencies of Open-Channel Noise and ⟨i⟩ Are Similar and Weak

Single-channel currents were recorded in different patches at different bath temperatures. Both the mean power spectral density of open-channel noise and ⟨*i*⟩ had a weak temperature dependence that was fitted quite well by a single Q_{10} value of 1.3, throughout the 3–40°C range (Fig. 6). At 40°C, patches broke down rapidly and gating transitions were more frequent than at 20°C. The two points at 39 and 40°C, with very large error bars both come from only five averaged open-state spectra; all other points come from >38 open-state spectra. A slope of 1.3 still gave the best fit if these 39 and 40°C points were excluded.

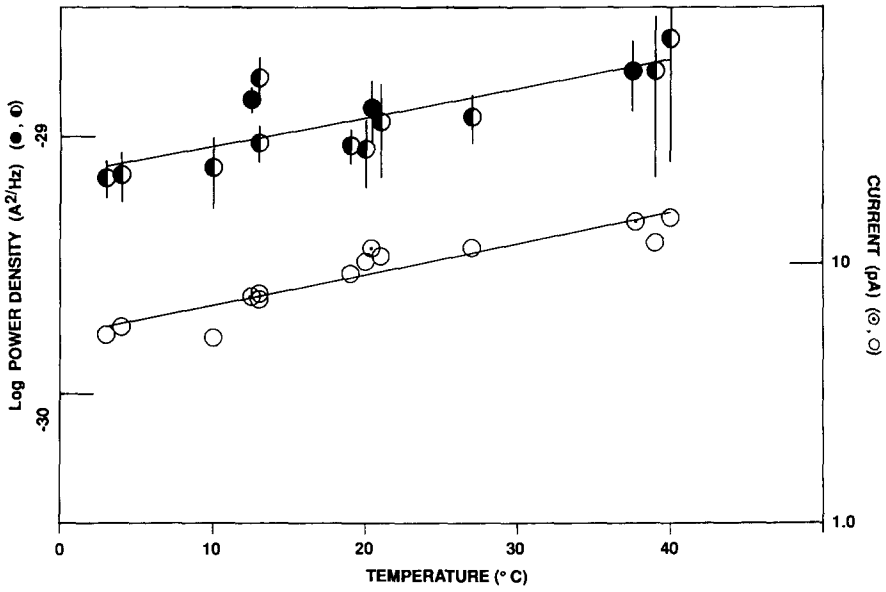

FIGURE 6. Mean power spectral density (*upper curve*) and ⟨*i*⟩ (*lower curve*) both increase weakly with temperature. Data from 11 patches with pipette voltage = +50 mV (*filled symbols*) or −50 mV (*open symbols*). The leftward ordinate shows log of mean power spectral density on the same scale as Fig. 5, the rightward ordinate shows the log of ⟨*i*⟩ (in picoamperes) both over two decades. The abscissa shows bath temperature on a linear scale. The solid lines are least squares fits to all points with equal weighting and both correspond to a constant Q_{10} of 1.3.

The observed weak temperature dependence of the measured power spectral density indicates that all spectral components present are stimulated weakly by increasing temperature. Though an apparently weak temperature dependence could be given by strong, opposing changes with increasing temperature over some limited range, high Q_{10} values are not likely to give canceling effects throughout the 3–40°C range. A Q_{10} of 1.3 in the decade 0–10°C is equivalent to an Arrhenius activation energy of 17 KJ/mol (Hille, 1992). Though the Q_{10} parameter need not be the same in different decades of temperature, no variation is detectable in the present case.

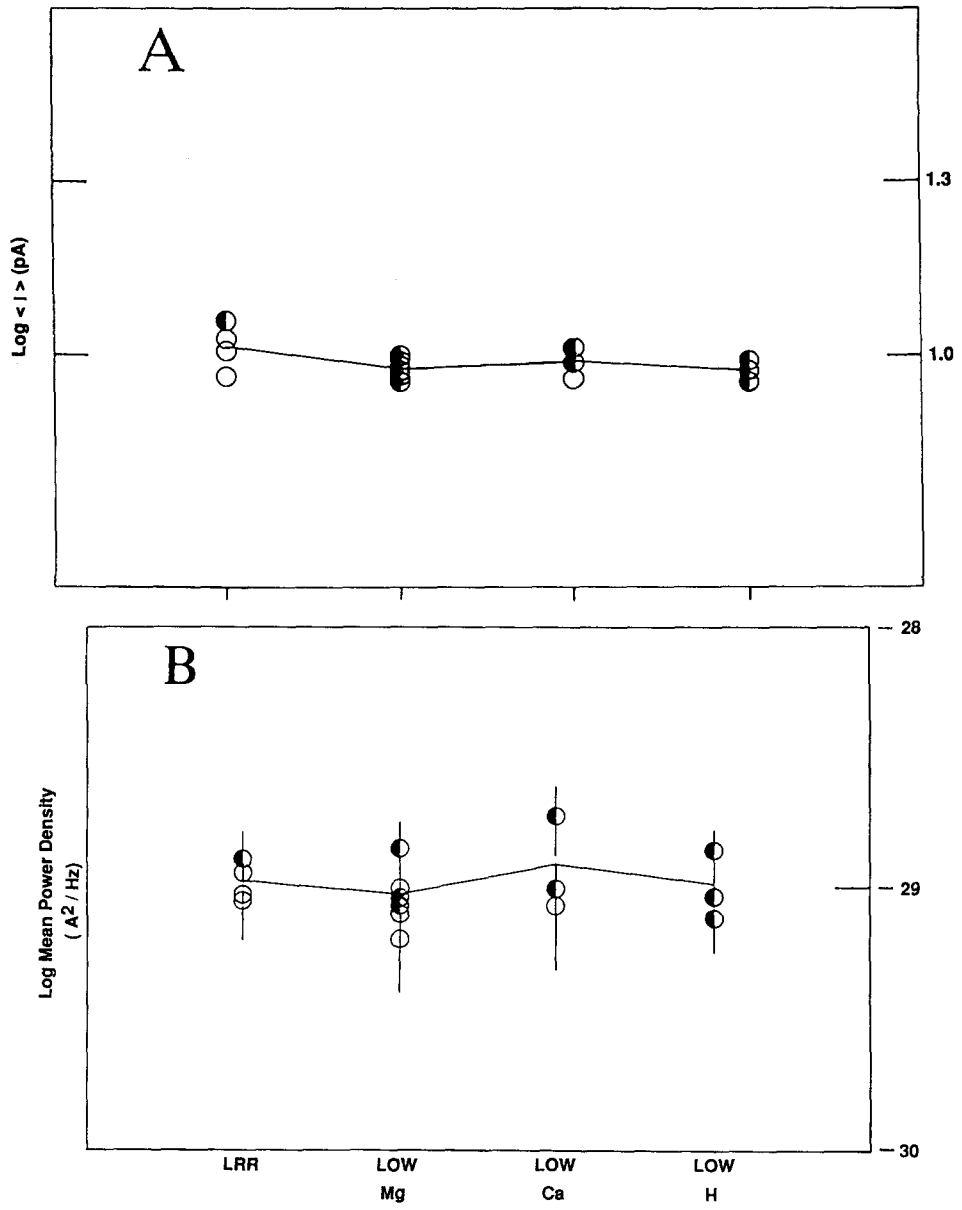

FIGURE 7. Effect of magnesium, calcium and hydrogen ions on mean current and the mean power spectral density of open-channel noise. Each symbol represents a different inside-out patch: control LRR data (four patches) low Mg (6) low Ca (3) low H (3). Pipette voltage = +50 mV (*filled symbols*) or −50 mV (*open symbols*). Means of all values in a column, equally weighted, are joined by solid lines. (*A*) Mean single-channel current, $\langle i \rangle$ (picoamperes) logarithmic ordinate over one decade. (*B*) Mean power spectral density (A^2/Hz), logarithmic ordinate over two decades.

Lines corresponding to a Q_{10} less than 1.0 or greater than 2.0 clearly do not agree with our data (not shown): a Q_{10} of 1.0 would give no increase with temperature; a constant Q_{10} of 2.0 would give a 16-fold increase (1.2 log U) between zero and 40°C.

Our observed Q_{10} of 1.3 for mean potassium conductance in this channel agrees with Coronado et al. (1980) and Shen, Hill, Rasmussen, and Strauss (1988). On the other hand, a $Q_{10} > 2$ is observed for most channel gating processes (for review, see Hille, 1992; Lee and Deutsch, 1990). In the canine cardiac SR potassium channel, a Q_{10} of 4.0 was found for a single-channel gating rate constant (Shen et al., 1988).

Aqueous Ions: Magnesium, Calcium and Hydrogen

With low Mg solution, bathing both sides of the channel, the mean power spectral density and $\langle i \rangle$ are very similar to those obtained with LRR. As low Mg solution contains only 5 μM total magnesium the measured power spectrum and mean current are clearly not affected by Mg^{2+} ions in the range 0.005–1.0 mM (Fig. 7). Complexed forms of magnesium such as Mg-ATP are also exonerated by this result. It was therefore considered permissible to pool data from recordings in LRR and low Mg solutions for kinetic analysis (below).

The true free Ca^{2+} present in low Ca solution due to impurities is unknown, but using 50 mM total calcium as an upper limit, we calculate 20 nM maximum free Ca^{2+}. Fibers did not survive for long in this solution and patch clamp recordings were poor. The mean power spectral density of open-channel noise recorded in low Ca showed no clear reduction and $\langle i \rangle$ was unchanged (Fig. 7) suggesting that the calcium present in LRR does not significantly affect the SR K channel. Further, low H solution contains 10 nM hydrogen ions and only 2 nM calculated free Ca^{2+} (due to the increased availability of unprotonated EGTA) and three patches in low H solution gave power spectra and $\langle i \rangle$ values that were not detectably different from those in LRR (Fig. 7). These results show that the measured open-channel noise is not affected by free Ca^{2+} in the range 10^{-9}–10^{-7} M, or by hydrogen ions in the range pH 7–pH 8. They also exonerate complexed forms of calcium, such as Ca-EGTA.

DURATIONS OF BRIEF CLOSINGS

This channel's openings contain many brief interruptions with a variety of amplitudes (Figs. 1, 9). Here, the kinetics of brief full closings and 80% amplitude substates are investigated. Missed events of these two types were thought most likely to produce open-channel noise, full closings by virtue of their amplitude and 80% substates by virtue of their frequent occurrence.

Duration histograms show two well-separated exponential populations of brief, full closings (Fig. 8). One component was fitted by simple least squares regression to the semi-logarithmic histograms in the range 200–800 μs (Fig. 8 *A*). This slow component was subtracted and a second, fast component fitted to the remainder in the range 40–150 μs (Fig. 8 *B*). Data pooled from five recordings with either LRR or low Mg solution in bath and pipette give a mean fitted time constant and event frequency for the slow component: $\tau_1 = 220 \pm 60$ μs and $\lambda_1 = 10 \pm 6$ events per second, respectively (mean, SD, $n = 5$); for the fast component, $\tau_2 = 28 \pm 4$ μs and $\lambda_2 = 62 \pm 20$ s^{-1} ($n = 5$).

Duration histograms for brief full closings may be contaminated by extraneous

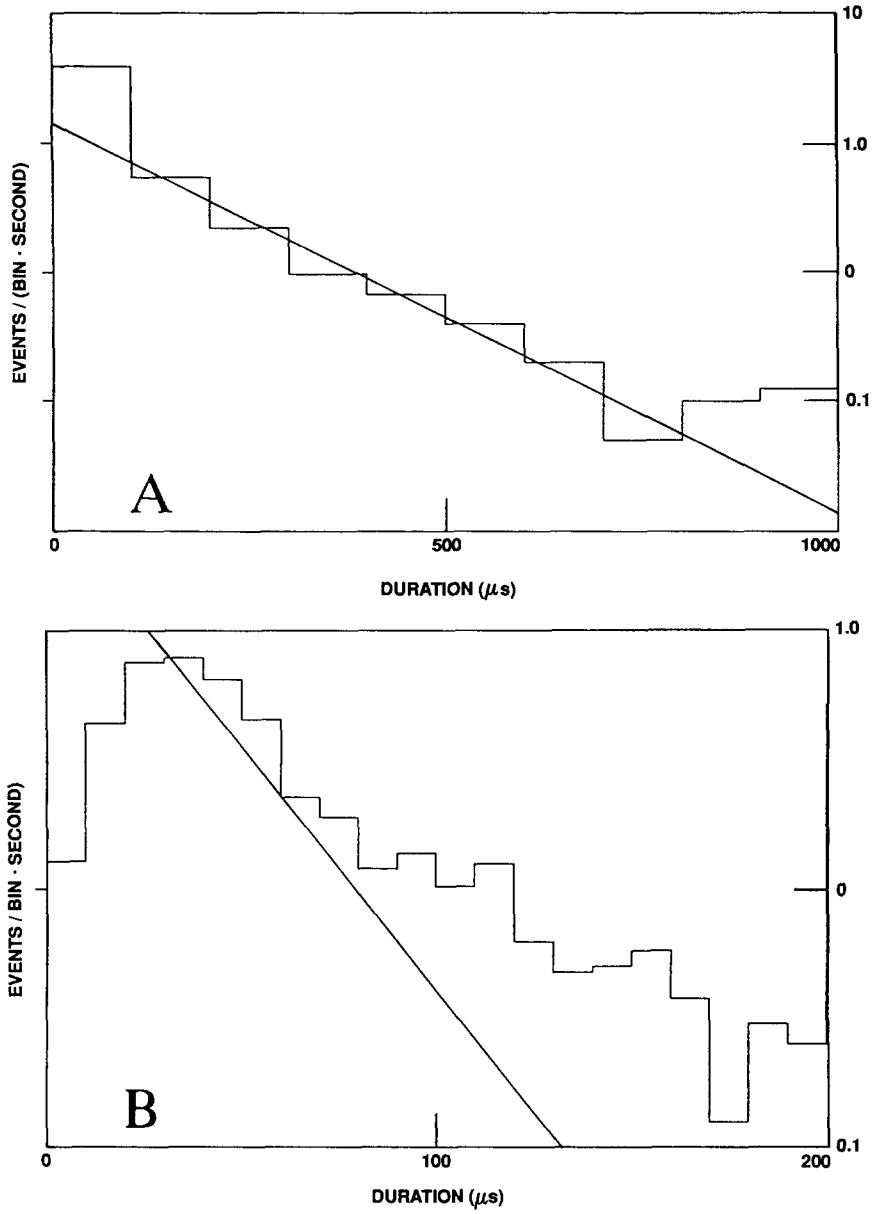

FIGURE 8. Semilogarithmic duration histograms of brief, full closings from a patch in low Mg solution, pipette voltage = +50 mV. (*A*) Duration histogram of ~2,000 events over a period of 40 s, number of events per second per bin (logarithmic scale, four decades) vs event duration in μs (linear scale). (*B*) Expanded view of the first two bins of *A* (ordinate: two decades; 10 μs/bin). Events briefer than 20 μs are not expected to reach the threshold for detection. Two exponential components were assumed to be present (see text). The fitted slow component is shown in *A*, the fast component in *B* (*straight lines*).

events, such as far-reaching open-channel noise excursions and substates of amplitude 0–50% of the main open state. Spurious threshold crossing by noise excursions is very unlikely as $\langle i \rangle$ = 9 pA and the RMS noise is ~0.5 pA, hence, the threshold lies ~9 RMS distant. Threshold crossing by substates is likely, however. To investigate this possibility, the durations of 158 full closings were determined by eye, on inspection of 10 s of contiguous data from a given patch. Only events that reached the fully closed amplitude were accepted, and the half-amplitude duration determined with a manually-placed cursor. The duration histogram of these events was too sparse to be fitted adequately but the number of events observed in a given duration range could be compared with that predicted from the duration histograms obtained by the automated process. Integrating Eq. 1 and using the mean fitted values of τ and

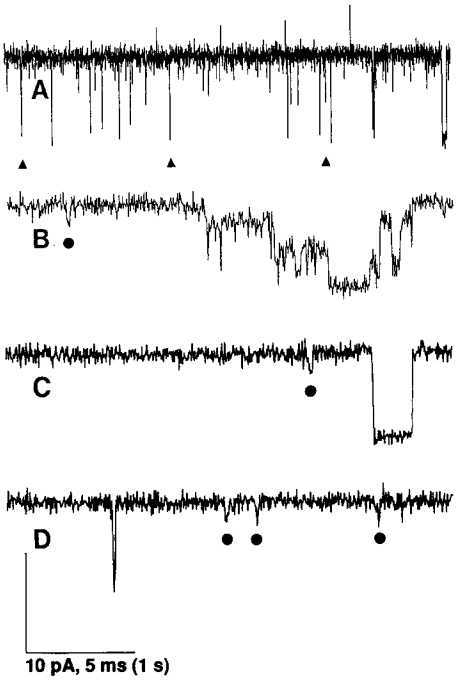

FIGURE 9. Brief 80% substates. (*A*) 4.5 s of data from a patch in low Mg solution, pipette voltage = +50 mV. Downward deflections indicate closings ($\langle i \rangle$ = 9.0 pA). The prominent upward deflections are caused by the switch that discharges the feedback capacitor in the patch clamp headstage. The open-channel noise RMS is ~0.5 pA. (*B–D*) Selected 20-ms periods (whose locations are marked by arrowheads in *A*) at high resolution (5 μs/point) to show brief 80% substates. Filled dots mark long-lived examples. For comparison, the full closing in *D* is 100 μs wide at half-maximal amplitude. *B* shows three subconductance levels (of roughly 80, 50, and 30% amplitude). Such short-lived periods of paroxysmal jumping between states are seen in all recordings.

λ given above, 106 events were predicted in the 50–100 μs range (92 from the fast component, 14 from the slow). Only 65 were seen, 61% of the predicted number. Similarly, 40 events were predicted in the 100–200 μs duration range (19 from the fast component, 21 from the slow). Only 33 were seen (83%). This sample of manually fitted durations suggests that the automated process overestimates the number of full closings. As several substates of 0–50% amplitude are observed in the single-channel records, these are almost certainly the source of this error.

Durations of Brief 80% Substates

Many brief 80% substates are seen in time domain records at high band width (Fig. 9). These are the channel's smallest recognizable interruptions and also the most

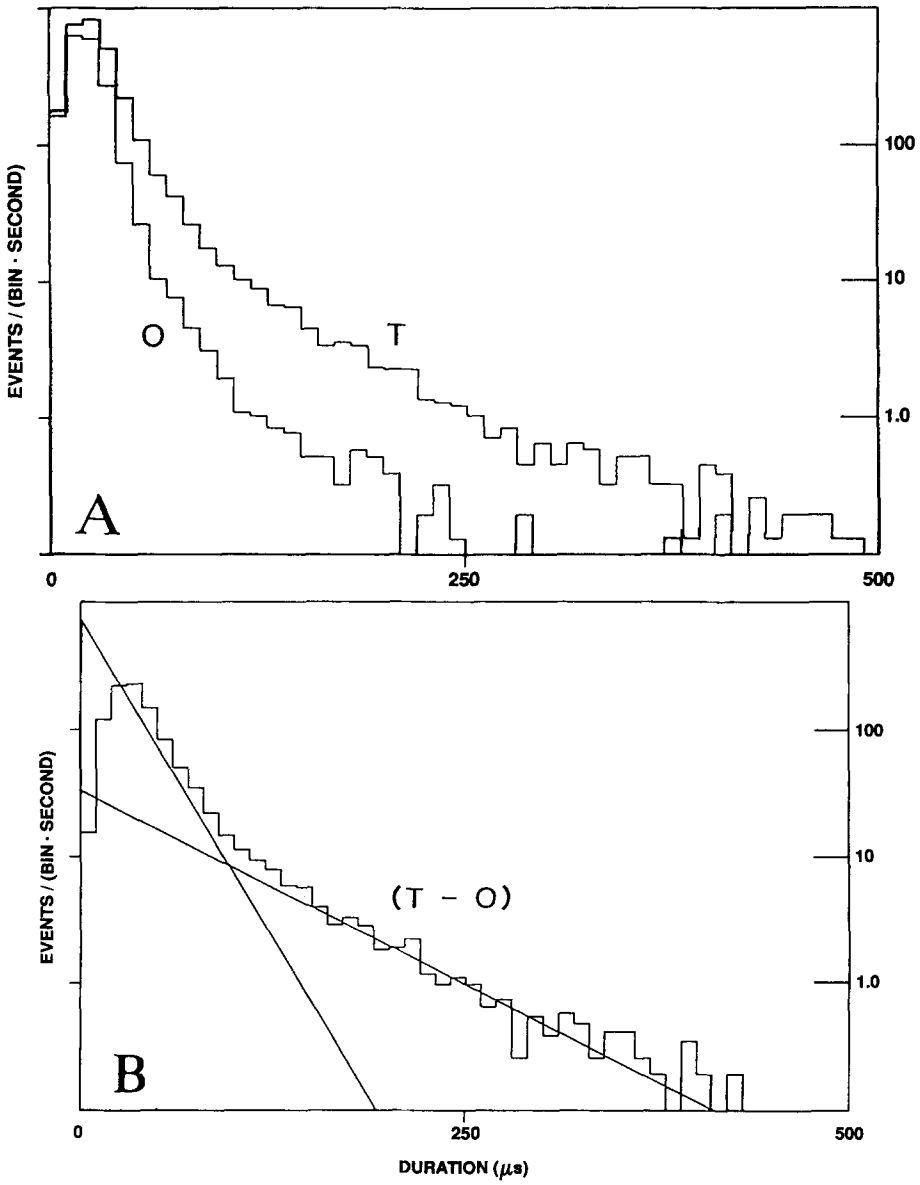

FIGURE 10. Semilogarithmic duration histograms of brief 80% substates (~2 pA in amplitude) in 15 s of data from the same recording as in Fig. 9. Number of events per second per bin (logarithmic scale, four decades) vs event duration in microseconds (linear scale, 10-μs bins). (*A*) Durations of brief, small excursions (10–30% of $\langle i \rangle$) from the main conductance state, either in the direction opposite (*O*) to the closed state, or towards it (*T*). In the former, 28,000 durations were sampled, and 43,000 in the latter. (*B*) The result of subtracting the two histograms in *A*, is an estimate of the duration histogram of brief 80% substates. Two exponential components were fitted, drawn as straight lines in *B*.

frequent ($\sim 1{,}000\ s^{-1}$). Being small and brief, they are likely to be missed by the masking program, are hard to distinguish from background noise spikes and are poorly resolved in amplitude histograms. Using the subtraction process described in Methods (see Fig. 10) duration histograms for these substates were made from three patches, two in Low Mg, one in low H solution. In all three there was clearly more than one population of dwell times (Fig. 10 *B*) and histograms were fitted with two exponential components, as before. A slow component was fitted in the range 150–300 μs. This was then subtracted and a fast component fitted in the range 50–150 μs. The mean fitted parameters are $\tau_3 = 69 \pm 3$ μs and $\lambda_3 = 240 \pm 15\ s^{-1}$ for the slow component, and $\tau_4 = 22 \pm 1$ μs and $\lambda_4 = 1{,}200 \pm 400\ s^{-1}$ for the fast component (mean, SD, $n = 3$). Bins decline for durations <30 μs indicating that events were missed. As the fast component dominates the histogram for a few bins only and depends heavily on the subtraction process, its parameters are uncertain, although similar results were obtained from all three patches. The fitted parameters are not substantially altered ($<30\%$ difference in any parameter) if the bin width is 20 rather than 10 μs (not shown).

The results obtained by the above automated process were compared with 400 durations determined by eye. Only events that clearly reached 80% amplitude were accepted, and the half-amplitude duration determined with a manually placed cursor. Using the mean fitted parameters from the automated process, 260 events are predicted in the 50–100 μs duration range (170 from the fast component, 90 from the slow) and only 157 such events were seen (60%). Likewise, 85 events are predicted in the 100–200 μs duration range (20 from the fast component, 65 from the slow) and only 41 were seen (48%). Again, the automated process clearly overestimates the number of brief 80% substates, not only from the fast component, but also from the well-fitted slow component. Even if the fitted slow component were correct, it alone cannot explain the number of brief events found by eye: a faster component must also be present. The duration histogram subtraction method, which has little effect above 50 μs, is unlikely to cause the disagreement. It is more likely that the computer-determined histograms are inflated by substates of 60–90% amplitude.

DISCUSSION

Is the Measured Power Spectrum Due to Discrete-Transport Noise Alone?

The low, constant power spectral density and its weak temperature dependence, similar to that of $\langle i \rangle$, suggested that discrete transport noise might be the dominant source of open-channel noise: for three reasons, it cannot be the only source. First, the measured power spectral density is too high according to the usual theory of discrete transport noise. At 50 mV (20°C), the measured power spectral density is $10.7 \times 10^{-30}\ A^2/Hz$. The range of possible values for the power spectral density of discrete transport noise is $2.9 - 5.8 \times 10^{-30}\ A^2/Hz$, given by Eqs. 19 and 20. Thus, the expected discrete transport noise could account for 27–54% of the measured value at 50 mV. Second, the variation of mean power spectral density with $\langle i \rangle$ is too steep (Fig. 5). A limiting slope is not reached, but a slope of 2 is approached with the highest values of $\langle i \rangle$ measured, as is best seen by considering only the seven right-hand points in Fig. 5. Discrete transport noise is expected to approach a slope

of 1.0 in the limit of high $\langle i \rangle$, in accordance with the Schottky formula (Eq. 15) as the unitary current events approach a Poisson process (see Appendix IV). Third, missed brief interruptions are responsible for some fraction of the measured power spectral density (see below).

Conductance Fluctuations as a Source of Excess Noise

The power spectral density of current noise caused by fluctuations in channel conductance will rise steeply with $\langle i \rangle$, ideally in proportion to $\langle i \rangle^2$ (Appendix I). This is compatible with the observed small excess over the Johnson formula value for low values of $\langle i \rangle$, progressively increasing as $\langle i \rangle$ increases (Fig. 5). Three possible physical mechanisms are the following: (*a*) vibrational motion within the channel molecule giving continuous variation in the potential energy profile of the conducting pathway, leading to continuous conductance fluctuations; (*b*) maintained conformational changes in the channel molecule producing gating transitions; (*c*) temporary blockage of the open channel by an extrinsic agent, such as an ion in the aqueous solution.

Current noise due to fluctuations in the voltage across the channel must be very small here. The pipette resistance is <100 MΩ and the Johnson voltage noise of this resistance (van der Ziel, 1970) applied to a 180-pS channel, produces current noise with power spectral density $<5.2 \times 10^{-32}$ A^2/Hz, which is negligible. The contribution of surface charges to fluctuating transmembrane voltage is also likely to be negligible as the ionic strength of our solutions is close to 1 M and the Debye length is therefore very small. As our solutions contain 480 mM K^+, nearly 10-fold greater than the concentration for half-maximal conductance (Coronado et al., 1980), the channel is almost saturated in our hands. It therefore seems unlikely that any noise mechanism based on fluctuations in K^+ concentration close to the channel will apply here. Not negligible, on the other hand, are local fluctuations in voltage due to moving charges within the membrane and close to the channel. These charges would be shielded from the high ionic strength of the aqueous bathing solution and their electric field would be felt by the ion conducting pathway. The resulting fluctuations in the electrical potential profile of that pathway would produce a fluctuation in conductance and so are, formally equivalent (in that sense) to the conductance fluctuations considered in the last paragraph.

Random, apparently continuous conductance fluctuations are observed in the nicotinic AChR channel (Sigworth, 1985) with a symmetrical, Gaussian amplitude distribution. Their power spectrum has a low-frequency plateau with a corner frequency at ~300 Hz (Sigworth, 1985) and was interpreted as a Lorentzian. A similar result is observed in a stretch-activated cation channel in frog lens epithelium, with corner frequency of ~1 kHz (Eisenberg et al., 1987). The SR potassium channel has no corner frequency in the 100 Hz–10 kHz range, with $\langle i \rangle$ between 2 and 15 pA, applied voltages of 20–70 mV, and bath temperatures of 3–40°C. If continuous conductance fluctuations were present, they would be missed by the masking program and a corner frequency would be seen in the power spectrum. We therefore exclude any but a minor contribution from continuous fluctuations with a corner frequency below 10 kHz.

We cannot exclude similar fluctuations with a much greater corner frequency, so that only the low-frequency plateau is seen in all measured spectra. Our data require

first that the low-frequency plateau must increase steeply with $\langle i \rangle$, in approximately second-power fashion and second, that it must increase weakly with temperature, with a Q_{10} close to 1.3. Previous results suggest that these are reasonable requirements. In both the nicotinic channel (Sigworth, 1985) and the stretch-activated channel (Eisenberg et al., 1987) the low frequency plateau increased steeply with $\langle i \rangle$. In neither case did the plateau increase with $\langle i \rangle^2$, but with a slightly lower power-law dependence (1.5–1.8), attributed to voltage sensitivity of the underlying conductance fluctuations [of $S_g(f)$ in Eq. 5]. In the nicotinic channel, a low temperature dependence is deduced for the low frequency plateau, in that the normalized variance ($\sigma_L^2/\langle i \rangle^2$) and the corner frequency (f_c) had Q_{10} values of 1.1 and 3.4 respectively (Sigworth, 1985). Using a Q_{10} of 1.7 for $\langle i \rangle$ (from Sigworth, 1985, Fig. 4) gives a Q_{10} of 3.2 for σ_L^2 and ~ 1.0 for $S_L(0)$ from Eq. 7. A strong temperature dependence of σ_L^2 and f_c then, presumed to reflect conformational changes in the protein, need not be accompanied by a strong temperature dependence of $S_L(0)$. Thus, the above two requirements are met in the nicotinic channel for fluctuations of $\backsim 300$ Hz and may also apply to fluctuations with a corner frequency > 10 kHz. Hence, whether or not they are the dominant source of noise, continuous fluctuations with a corner frequency above 10 kHz and small amplitude cannot be excluded by our results.

Fast Block by Aqueous Ions Does Not Add Significant Noise

We hoped to reduce the power spectral density by removing possible aqueous blockers from the bathing solution, specifically magnesium, calcium, and hydrogen ions. The magnesium ion blocks a number of biological channels (Stanfield, 1988, for review) and significant reduction of NMDA currents occurs even with 10 μM Mg^{2+} (Nowack, Bregestovski, Ascher, Herbet, and Prochiantz, 1984). Miller (1978) found that Mg^{2+} inhibited many channel currents of the rabbit-reconstituted SR potassium channel, with half-maximal effect at 4 mM. Our results, however, indicate that the 1 mM free Mg^{2+} present in LRR has no effect on open-channel noise. We also find no obvious effect of Mg^{2+} either on $\langle i \rangle$ or on the channel's kinetics, suggesting that the lobster channel is less sensitive to Mg^{2+} than the rabbit channel.

The absence of effect of low Ca and low H solutions on the mean power spectral density indicates that neither free nor complexed calcium ions, nor hydrogen ions significantly affect open-channel noise under the conditions used. Blockade mediated by calcium ions with a half-maximal concentration below 2 nM is most unlikely. Given the identical results at pH 7 and pH 8, hydrogen ion-mediated block with a pK_a well above 8 might be suggested, perhaps involving one of the basic amino acids (e.g., lysine, $pK_a = 10.5$ in aqueous solution). Considering a simple binding reaction, H^+ (aq) + R → HR, where the bound state HR corresponds to the blocked state of the channel, we require that the dissociation constant for this reaction, given by $K_D = k_{off}/k_{on}$, be less than 10^{-8} M. Using the unusually high value of k_{on} found by Prod'hom, Pietrobon, and Hess (1987) for the association rate constant of hydrogen ions as an upper bound, $k_{on} < 4 \times 10^{11}$ M^{-1} s^{-1}, we deduce that k_{off} must be $<$ 4,000 s^{-1}. This in turn requires a time constant τ ($=1/k_{off}$) that is > 250 μs, corresponding to the average lifetime of the hydrogen-bound state HR. An exponential population with $\tau > 250$ μs would be readily detectable under the present

recording conditions and most such events would be removed by the masking program. In addition, the number of events detected should decrease greatly on replacing pH 7 with pH 8 LRR. No such effect was observed and brief blockages mediated by hydrogen ions are ruled out as a possible source of open-channel noise.

The only remaining possible blockers are HEPES, chloride and glutamate itself. Block of the SR K^+ channel by anions seems improbable, but the glutamate ion has a primary amine group that is protonated in LRR ($pK_a = 9.6$) and might act as a blocker. A power spectrum obtained from currents recorded in LRR in which glutamate was replaced by gluconate (which has no amine group) was very similar to those obtained with conventional LRR (not shown) suggesting that glutamate does not affect open-channel noise. We cannot exclude the possibility of an unidentified aqueous species, consistently present as an impurity in our bathing solutions, producing brief blockages of the channel.

Open-Channel Noise from Truncated Exponentials

Interruptions of the single-channel current that are much briefer than the rise time of the recording system will be buried in the Gaussian background noise and not detected by the masking program, but will still add to the measured open-channel noise (see Appendix III). The long openings of this channel contain several populations of brief interruptions, each presumed to have an exponential distribution of lifetimes. Missed events from each population will give a finite power spectral density, as described by Eq. 11. We have calculated this for two types of brief interruption that seemed likely to be significant sources of open-channel noise: brief closings and substates of 80% amplitude. The maximum lifetime, D, for which each type of event would be missed by the masking program was estimated by applying square pulses of decreasing duration to the patch clamp input using a signal generator. The value of D was taken to be the duration of the first pulse whose peak failed to cross the threshold for masking. This threshold was 2.5 standard deviations (usually ~ 1.5 pA) away from the main conductance level. For brief full closings, D was 7 μs. Using Eqs. 11–13 with the mean fitted kinetic parameters given in Results, both exponential populations of brief full closings were calculated to add negligible open-channel noise: the faster component accounts for $< 1\%$ of the measured power spectral density, the slower $< 0.01\%$.

Brief excursions to the 80% substate are much more likely to be missed by the masking program than are full closings, and D was estimated to be ~ 30 μs for these events. Using the two fitted exponential components, Eq. 11 predicts a power spectral density of 1.3×10^{-30} A^2/Hz due to the fast component and 0.2×10^{-30} A^2/Hz due to the slow component. These events therefore account for a small fraction ($\sim 14\%$) of the observed power spectral density at 50 mV, 20°C. As shown in Results, the frequency of these 80% substates is probably overestimated, by a factor of as much as two. The extraneous events underlying this elevation are likely to be larger in amplitude than the 80% substates and thus are less likely to be missed by the masking program. Hence the fraction given here (14%) is probably an upper estimate.

Speculations

Identified sources cannot completely account for the open-channel noise measured here. With a voltage of 50 mV, discrete transport noise is thought to underlie 27–54% of the power spectral density and less at higher voltages. Identified brief interruptions account for a small fraction (~14%). Thus, a significant fraction of the measured power spectral density, possibly the largest, is due to unidentified conductance fluctuations, rolling off above 10 kHz under all the conditions studied here. As all likely aqueous blockers have been excluded, a fluctuation process within the channel molecule itself is inferred. Two possible models for the hypothesized excess noise are the following.

First, as shown above, fast continuous conductance fluctuations are compatible with our data and are presumed to give a Lorentzian power spectrum. The power spectral density measured here imposes an upper limit on the low frequency plateau of $\sim 5 \times 10^{-30}$ A^2/Hz. In a 10-kHz band width, this upper limit corresponds to noise fluctuations with an RMS value of $\sigma < 0.2$ pA (<2.5% of $\langle i \rangle$). Such small scale wandering would not be detectable by eye. As no spectra rolled off below 10 kHz over the 3–40°C temperature range, we assume a lower limit for the corner frequency, $f_c > 10$ kHz. Substituting $f_c = 10$ kHz and $S_L(0) < 5 \times 10^{-30}$ A^2/Hz into Eq. 7 gives a maximum RMS value of $\sigma < 0.3$ pA, roughly 3% of $\langle i \rangle$.

Second, a fast gating process could also account for the observed power spectral density. Here again, the expected power spectrum is Lorentzian, $S_L(0)$ and f_c being given by Eqs. 9 and 10. For example, using the above lower limit $f_c > 10$ kHz, a low frequency plateau of $S_L(0) = 5 \times 10^{-30}$ A^2/Hz would be given by a single-exponential population of 90% amplitude substates (amplitude $a = 1$ pA at 50 mV) with $\tau < 16$ μs and $\lambda > 5{,}000$ s^{-1}. The same value of $S_L(0)$ would also be given by complete closures ($a = 9$ pA) with a more remote corner frequency limit $f_c > 100$ kHz, equivalent to $\tau < 1.6$ μs and $\lambda > 6{,}000$ s^{-1}. An upper limit on f_c is given by the constraint of nonzero open probability, i.e., $\lambda\tau < 1$. Using Eq. 9, for full closings, with $S_L(0) = 5 \times 10^{-30}$ A^2/Hz, this constraint gives $\tau > 15$ ns, or from Eq. 10, $f_c < 10^7/Hz$. This upper limit is, as expected, less than the net transport rate of 5×10^7 ions per second (given by $\langle i \rangle = 9$ pA). Our requirement that the corner frequency of the proposed conductance fluctuations be in the range 10^4–10^7 Hz is well within the wide range over which motions in proteins are known to occur (Brooks, Karplus, and Pettitt, 1988).

If the observed noise is due to motion within the channel molecule, it is slightly surprising that the measured power spectral density has such a consistently weak temperature dependence. As noted above, Gaussian continuous noise due to conformational fluctuations in the nicotinic channel gives a corner frequency that varies strongly with temperature but a low frequency plateau that varies hardly at all (Sigworth, 1985). If similar continuous fluctuations underlie the excess noise in our channel then the observed weak temperature dependence may arise in the same way. Nevertheless, if a fast gating process is the correct model for our excess noise then Eq. 9 would describe its power spectral density and it is surprising that the quantity $4\lambda\tau^2\alpha^2$ should maintain a constant Q_{10} of 1.3 over the wide range 3–40°C. The temperature sensitivity of α is likely to be very similar to that of $\langle i \rangle$. By contrast, the

relatively slow range 10^{-8}–10^{-5} s for τ (equivalent to the range 10^4–10^7 Hz for f_c, from Eq. 10) suggests that the underlying reaction is a transition between maintained conformational states. Such a transition will by definition involve high energy barriers—higher than those of the ionic diffusion process underlying $\langle i \rangle$—and therefore will exhibit a high temperature dependence, higher than that of $\langle i \rangle$. Although low temperature-dependencies have been reported for the RMS displacement of surface sidechain carbon atoms in myoglobin, measured by x-ray scattering, the underlying motion has a characteristic frequency much greater than 10^7 Hz (Frauenfelder, Petsko, and Tsernoglou, 1979) and we have found no reported example of protein fluctuations in the range 10^4–10^7 Hz with low temperature dependence. This paradox of low corner frequency (and implied high energy barrier) with low temperature dependence of $S_L(0)$ might be explained by results derived from the viscosity dependence of oxygen binding to myoglobin (Beece, Eisenstein, Frauenfelder, Good, Marden, Reinisch, Reynolds, Sorensen, and Yue, 1980). Rate constants in the range 10^5–10^8 s^{-1} (at 27°C) were measured for the series of reactions involved in access of O_2 from the surface of the protein to its target, the heme iron atom. In the range 0–40°C, these rate constants had temperature-dependencies equivalent to Q_{10} values between 1.8 and 3.3. Increasing solvent viscosity potently reduced the rate constants themselves without affecting their temperature sensitivity. Both enthalpic and entropic components of each reaction's activation energy were interpreted as being viscosity dependent (Beece et al., 1980). This demonstration that temperature sensitivity does not uniquely specify a rate constant may be relevant to our results. We speculate that a conformational change within some part of our channel molecule (*a*) occurs in a microenvironment of high viscosity and (*b*) causes conductance fluctuations that we measure as open-channel noise. The conformational change would have rate constants with a weak temperature dependence but the rate constants (and corner frequency) would be unusually low, thanks to the high local viscosity. This speculation recalls Läuger's (1985) fit to Sigworth's (1985) data, where channel subunits' motion was modeled by the Langevin equation with a very high viscosity term. In conclusion, the observed weak temperature dependence is not necessarily at odds with the notion of conformational fluctuations in the range 10^4–10^7 Hz being the underlying source of excess noise.

APPENDIX

On Noise Mechanisms

I. General conductance fluctuations. For a stationary fluctuating conductance $g(t)$ in a constant voltage V the current at any instant is:

$$i(t) = Vg(t). \tag{2}$$

The mean current and the power spectral density of the current fluctuations are then by definition:

$$\langle i \rangle = V\langle g \rangle \tag{3}$$

$$S_i(f) = V^2 S_g(f) \tag{4}$$

where $S_g(f)$ is the power spectral density of the conductance fluctuations. Thus,

$$S_i(f) = (\langle i \rangle^2 / \langle g \rangle^2) S_g(f). \tag{5}$$

II. Lorentzian processes. A Lorentzian power spectral density is defined as

$$S_L(f) = S_L(0)/[1 + (f/f_c)^2] \tag{6}$$

where $S_L(0)$ is the power spectrum's low frequency plateau and f_c is its corner frequency. The variance of any Lorentzian process is given by:

$$\sigma_L^2 = \pi S_L(0) f_c / 2. \tag{7}$$

It was very reasonable to assume that the Lorentzian equation (Eq. 6) described the observed spectra of Sigworth (1985) and Eisenberg et al. (1987). Any Markovian random variable $x(t)$ whose mean evolves linearly over time (i.e., $d\langle x(t) \rangle / dt = -k\langle x\ (t) \rangle$ where k is constant, maybe zero) will have an exponential correlation function in the time domain (Nelsen, 1987) and hence a Lorentzian power spectrum. Here $x(t)$ is the channel's conductance. These conditions are broad and many noise processes have a Lorentzian power spectrum.

III. Open-channel noise due to brief interruptions. A square pulse of current of amplitude a and duration d has a power spectrum $S_P(f)$ given by

$$S_P(f) = a^2 \sin^2 (\pi df)/(\pi f)^2. \tag{8}$$

A very brief pulse has a power spectrum that is practically constant ($\sim a^2 d^2$) up to some very high frequency ($\sim 1/2\ d$). The limited rise time of the recording system simply acts as a low-pass filter and preserves all the low-frequency components of the pulse's power spectrum. Brief interruptions, due either to gating of the channel molecule itself or to block by an extrinsic agent, form a binary sequence of pulses, with exponentially distributed dwell times in the open and closed states. The power spectrum of such a binary sequence is a Lorentzian (Papoulis, 1984) given by Eq. 6. For very brief interruptions, none of which is resolved, the power spectral density measured would be the low-frequency plateau, well approximated by:

$$S_L(0) = 4\lambda\tau^2\alpha^2 \tag{9}$$

where λ is the average rate of occurrence of brief interruptions, and τ is their average duration, equal to the time constant of the exponential distribution of lifetimes. The true amplitude of the interruptions is a, and we define $\alpha = a\ (1 - \lambda\tau)$. For full closings, α is the observed mean current, $\langle i \rangle$. The rate constants for this binary process are given by $1/\tau$ and $\lambda\ (1 - \lambda\tau)$ (closed $\rightarrow$ open *and* open $\rightarrow$ closed, respectively). The closing rate constant is very close to λ, and α is very close to a, if $\lambda\tau$ is much less than 1, as it always is here. The corner frequency and time constant are related by:

$$f_c = 1/(2\pi\tau). \tag{10}$$

If the interruptions are not much briefer than the recording system's resolution, then only a fraction of them, the briefer ones, will be unresolved and missed by the

masking program. The power spectral density, $S_T(f)$, of such missed events is again practically constant in the measurable frequency range. For a given exponential population of lifetimes, $S_T(f)$ is calculated from the τ and λ values for the distribution, which are estimated from measured duration histograms in the range where lifetimes can be reliably determined (Sigworth et al., 1987):

$$S_T(0) = 2\lambda_T\langle t_T^2\rangle a^2, \tag{11}$$

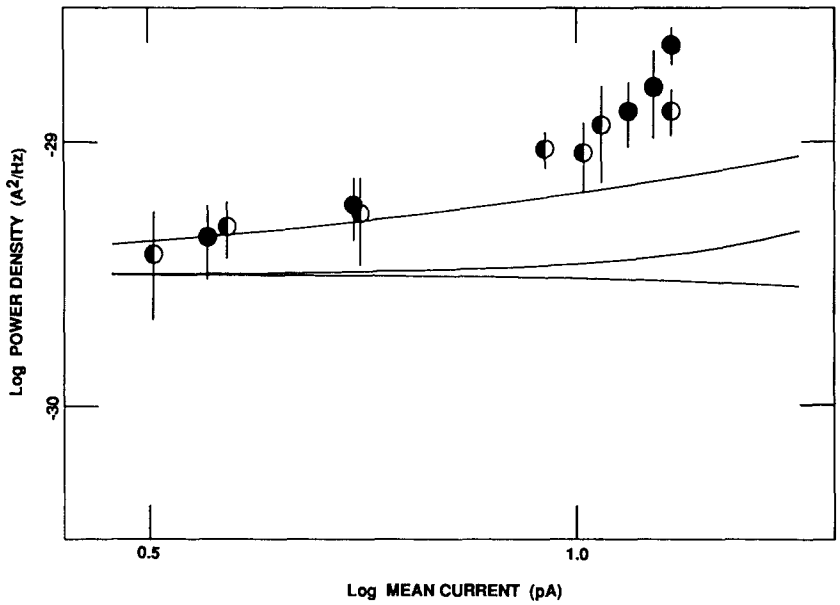

FIGURE 11. Prediction of discrete transport noise for a particular model of the SR potassium channel. Data points are from Fig. 5, with the same axes. The lowest solid line shows the Johnson formula value (Eq. 14) assuming a constant mean single-channel conductance of 180 pS at 20°C. The top solid line shows the sum of the Johnson and Schottky formula values (Eq. 19). The middle line shows the prediction of Frehland's (1978) method, using rate constants derived from Coronado et al. (1980).

where λ_T is the mean frequency of missed events and $\langle t_T^2\rangle$ is their mean squared duration. These parameters are calculated from the truncated exponential density of the lifetimes of brief interruptions:

$$\lambda_T = \frac{\lambda}{\tau}\int_0^D \exp(-t/\tau)dt \tag{12}$$

$$\langle t_T^2\rangle = \frac{\lambda}{\tau}\int_0^D t^2 \exp(-t/\tau)dt, \tag{13}$$

where D is the maximum lifetime missed (i.e., the longest event contributing to the measured power spectral density).

IV. Discrete transport noise. Discrete transport noise arises in any electric current as a result of random thermal motion of the discrete charged particles that carry the current. The power spectral density, S_d, of discrete transport noise is described by two simple formulae under precisely defined conditions (Oliver, 1965; van der Ziel, 1970). First, for any conductance, g, at equilibrium, the Johnson (thermal) noise formula gives

$$S_d = 4kTg \tag{14}$$

up to some very high frequency, where k is Boltzmann's constant and T is absolute temperature. Second, for a current that is made up of a stationary train of identical pulses, occurring independently of each other (a Poisson process) the Schottky (shot) noise formula gives:

$$S_d = 2q\langle i\rangle \tag{15}$$

where $\langle i\rangle$ is the mean current and q is the charge equivalent to one unitary pulse (its integral over time). The spectrum must roll off at some very high frequency of the order of $1/d$, where d is the duration of the unitary pulses. Discrete transport noise in an ion channel is expected to obey the Johnson formula with identical solutions in both baths and $\langle i\rangle = 0$. It is expected to obey the Schottky formula at such a high voltage that ion transit events are effectively unidirectional, and such a low concentration that they are independent of each other.

For intermediate voltages, there is no general formula for S_d. It will depend on the details of the ion transport process. To obtain a reasonable upper bound on S_d for intermediate $\langle i\rangle$, we assume that S_d increases most steeply with increasing $\langle i\rangle$ in the limit of high $\langle i\rangle$, when the Schottky formula is obeyed. By definition, for any function $y(x)$, integrated between the limits a and b:

$$y(b) = \int ab \frac{dy(x)}{dx} dx + y(a). \tag{16}$$

If $y(x)$ is $S_d(\langle i\rangle)$ and the limits are $a = 0$ and $b = j$, where j is some intermediate value of $\langle i\rangle$, then:

$$S_d(j) = \int_0^j \frac{dS_d}{d\langle i\rangle} d\langle i\rangle + S_d(0). \tag{17}$$

As noted above, the maximum value of the integrand is assumed to be that given by differentiating Eq. 15, and $S_d(0)$ is given by Eq. 14. Hence:

$$S_d(j) < \int_0^j 2qd\langle i\rangle + 4kTg \tag{18}$$

$$S_d(j) < 2qj + 4kTg. \tag{19}$$

We thus obtain the sum of the Johnson and Schottky formula values as an upper bound on S_d for intermediate $\langle i\rangle$. The lowest possible value for S_d in a given conductance is assumed to be that given by the Johnson formula. Thus,

$$S_d(j) > 4kTg. \tag{20}$$

Violations of this rule (Eq. 20) are predicted for some semiconductors (Van der Ziel, 1970) but we know of none in practice.

The only general method for predicting S_d for a given transport mechanism (Frehland, 1978) assumes that ions make instantaneous hops between a finite number of fixed binding sites, that the hops occur in a random, Markovian manner and that each hop contributes a pulse of displacement current in the bath, proportional to the electrical distance hopped. This method embodies the fact that the unitary pulses are not independent of each other, so single file transport and one-ion occupancy can be included. Fig. 11 shows the discrete transport noise predicted by Frehland's method for a particular model of the SR K channel. The potential profile used is that derived by Coronado et al. (1980) using standard Eyring rate theory to fit their current-voltage data to a two-site, one-ion channel model. As expected, it approaches the Johnson formula value at low voltages, approaches the Schottky formula at high voltages (>500 mV, not shown) and always remains within the bounds given by Eqs. 19 and 20.

It is a pleasure to thank Drs. F. S. Cohen and F. J. Sigworth for their help and advice throughout this work, Dr. J. M. Tang for teaching A. H. Hainsworth the lobster preparation, Dr. S. B. Hladky for comments on the manuscript and Dr. C. M. Dobson, of the Inorganic Chemistry Laboratory, Oxford, for helpful discussion.

We are grateful for the steadfast support of the National Science Foundation.

Original version received 12 March 1992 and accepted version received 5 July 1994.

REFERENCES

Beece, D., L. Eisenstein, H. Frauenfelder, D. Good, M. C. Marden, L. Reinisch, A. H. Reynolds, L. B. Sorensen, and K. T. Yue. 1980. Solvent viscosity and protein dynamics. *Biochemistry.* 19:5147–5157.

Brigham, E. O. 1974. The Fast Fourier Transform. Prentice Hall, Inc., NY. 252 pp.

Brooks, C. L., M. Karplus, and B. M. Pettitt. 1988. Proteins: A Theoretical Perspective of Dynamics, Structure, and Thermodynamics. Advances in Chemical Physics. Vol. 71. John Wiley and Sons, Inc., NY. 259 pp.

Colquhoun, D., and F. J. Sigworth. 1983. Fitting and statistical analysis of single-channel records. *In* Single-Channel Recording. B. Sakmann and E. Neher, editors. Plenum Publishing Corp., NY. 191–265.

Coronardo, R., R. L. Rosenberg, and C. Miller. 1980. Ionic selectivity, saturation and block in a K^+ selective channel from sarcoplasmic reticulum. *Journal of General Physiology.* 76:425–446.

Eisenberg, R. S., A. H. Hainsworth, and R. A. Levis. 1987. Open-channel noise in a cation channel of frog lens epithelium. *Journal of Physiology.* 396:84P. (Abstr.)

Eisenberg, R. S., A. H. Hainsworth, and R. A. Levis. 1988. Open-channel noise in the potassium channel of lobster sarcoplasmic reticulum. *Journal of Physiology.* 407:101P. (Abstr.)

Eisenberg, R. S., A. H. Hainsworth, and R. A. Levis. 1989. The effect of temperature on open-channel noise in the potassium channel of lobster sarcoplasmic reticulum. *Journal of Physiology.* 410:18P. (Abstr.)

Frauenfelder, H., G. A. Petsko, and D. Tsernoglou. 1979. Temperature-dependent x-ray diffraction as a probe of protein structural dynamics. *Nature.* 280:558–563.

Frehland, E. 1978. Current noise around steady states in discrete transport systems. *Biophysical Chemistry.* 8:255–265.

Hainsworth, A. H. 1989. Open-channel noise in the large potassium channel of lobster sarcoplasmic reticulum. PhD thesis. Department of Physiology, Rush Graduate College, Chicago, IL.

Hainsworth, A. H., R. A. Levis, and R. S. Eisenberg. 1989. Excess open-channel noise in the SR K^+ channel: effects of temperature and Mg^{2+}. *Biophysical Journal.* 55:200*a*. (Abstr.)

Hainsworth, A. H., J. M. Tang, J. Wang, R. A. Levis, and R. S. Eisenberg. 1988. Open-channel noise in the K^+ channel of the sarcoplasmic reticulum. *Biophysical Journal.* 53:151a. (Abstr.)

Heinemann, S. H., and F. J. Sigworth. 1988. Open channel noise IV: estimation of rapid kinetics of formamide block in gramicidin A channels. *Biophysical Journal.* 54:757–764.

Heinemann, S. H., and F. J. Sigworth. 1989. Estimation of Na^+ dwell time in the gramicidin A channel. Na^+ ions as blockers of H^+ currents. *Biochimica et Biophysica Acta.* 987:8–14.

Heinemann, S. H., and F. J. Sigworth. 1990. Open channel noise V: fluctuating barriers to ion entry in gramicidin A channels. *Biophysical Journal.* 57:499–514.

Hille, B. 1992. Ionic Channels of Excitable Membranes. Sinauer Associates, Inc., Sunderland, MA. 607 pp.

Hladky, S. B. 1989. Models of ion permeation through membranes. *In* Ion Transport. D. Keeling and C. Benham, editors. Academic Press, NY. 263–278.

Kirlin, R. L., and A. Moghadamjoo. 1986. A robust running window detector and estimator for step signals in contaminated Gaussian noise. *IEEE Transactions on Acoustics, Speech and Signal Processing.* 34:816–823.

Läuger, P. 1985. Structural fluctuations and current noise of ionic channels. *Biophysical Journal.* 48:369–373.

Lee, S. C., and C. Deutsch. 1990. Temperature dependence of K^+-channel properties in human T lymphocytes. *Biophysical Journal.* 57:49–62.

Levitt, D. G. 1986. Interpretation of biological ion channel flux data—reaction rate versus continuum theory. *Annual Review of Biophysics and Biophysical Chemistry.* 15:29–57.

Miller, C. 1978. Voltage gated cation conductance channel from fragmented sarcoplasmic reticulum: steady state electrical properties. *Journal of Membrane Biology.* 40:1–23.

Miller, C., J. E. Bell, and A. M. Garcia. 1984. The potassium channel of sarcoplasmic reticulum. *Current Topics in Membranes and Transport.* 21:99–132.

Nelsen, R. B. 1987. Consequences of the memoryless property for random variables. *American Mathematical Monthly.* 94:981–984.

Nowak, L., I. P. Bregestovsk, P. Ascher, A. Herbet, and A. Prochiantz. 1984. Magnesium gates glutamate-activated channels in mouse central neurones. *Nature.* 307:462–465.

Oliver, B. M. 1965. Thermal and quantum noise. *Proceedings of the Institute of Electrical and Electronics Engineers.* 53:436–454.

Papoulis, A. 1973. Minimum bias windows for high resolution spectral estimates. *IEEE Transactions on Information Theory.* 19:9–12.

Papoulis, A. 1984. Probability, Random Variables, and Stochastic Processes. McGraw Hill, New York. 576 pp.

Prod'hom, B., D. Pietrobon, and P. Hess. 1987. Direct measurement of proton transfer rates to a group controlling the dihydropyridine-sensitive Ca^{2+} channel. *Nature.* 329:243–246.

Shen, W. K., J. A. Hill, R. L. Rasmusson, and H. C. Strauss. 1988. Temperature-dependent conductance of a canine cardiac sarcoplasmic reticulum K^+ channel. *Biophysical Journal.* 53:147*a*. (Abstr.)

Sigworth, F. J. 1985. Open channel noise I. Noise in acetylcholine receptor currents suggests conformational fluctuations. *Biophysical Journal.* 47:709–720.

Sigworth, F. J., D. W. Urry, and K. U. Prasad. 1987. Open channel noise III: high resolution recordings show rapid current fluctuations in gramicidin A and four chemical analogues. *Biophysical Journal.* 52:1055–1064.

Stein, P. G., T. E. Nelson, and P. T. Palade. 1989. Mammalian sarcoplasmic reticulum K channels recorded in skinned fibers. *Biophysical Journal.* 55:480*a*. (Abstr.)

Tang, J. M., J. Wang, and R. S. Eisenberg. 1989. K^+-selective channel from sarcoplasmic reticulum of split lobster muscle fibres. *Journal of General Physiology.* 94:261–278.

Van der Ziel, A. 1970. Noise: Sources, Characterization and Measurement. Prentice Hall, Inc., NY.